Human induced pluripotent stem cell-derived MGE cell grafting after status epilepticus attenuates chronic epilepsy and comorbidities via synaptic integration

Dinesh Upadhya[a,b,c,d,1], Bharathi Hattiangady[a,c,d], Olagide W. Castro[b,c,d,2], Bing Shuai[a,b,c,d], Maheedhar Kodali[a,b,c,d], Sahithi Attaluri[a,b,c,d], Adrian Bates[a,b,c,d], Yi Dong[e,f], Su-Chun Zhang[e,f,3], Darwin J. Prockop[a,b,c,3,4], and Ashok K. Shetty[a,b,c,d,3,4]

[a]Institute for Regenerative Medicine, Texas A&M Health Science Center College of Medicine, Temple, TX 76502; [b]Institute for Regenerative Medicine, Texas A&M Health Science Center College of Medicine, College Station, TX 77845; [c]Department of Molecular and Cellular Medicine, Texas A&M Health Science Center College of Medicine, College Station, TX 77845; [d]Research Service, Olin E. Teague Veterans' Medical Center, Central Texas Veterans Health Care System, Temple, TX 76504; [e]Waisman Center, Department of Neuroscience, School of Medicine and Public Health, University of Wisconsin–Madison, Madison, WI 53706; and [f]Waisman Center, Department of Neurology, School of Medicine and Public Health, University of Wisconsin–Madison, Madison, WI 53706

Contributed by Darwin J. Prockop, November 6, 2018 (sent for review August 19, 2018; reviewed by Detlev Boison and William P. Gray)

Medial ganglionic eminence (MGE)-like interneuron precursors derived from human induced pluripotent stem cells (hiPSCs) are ideal for developing patient-specific cell therapy in temporal lobe epilepsy (TLE). However, their efficacy for alleviating spontaneous recurrent seizures (SRS) or cognitive, memory, and mood impairments has never been tested in models of TLE. Through comprehensive video- electroencephalographic recordings and a battery of behavioral tests in a rat model, we demonstrate that grafting of hiPSC-derived MGE-like interneuron precursors into the hippocampus after status epilepticus (SE) greatly restrained SRS and alleviated cognitive, memory, and mood dysfunction in the chronic phase of TLE. Graft-derived cells survived well, extensively migrated into different subfields of the hippocampus, and differentiated into distinct subclasses of inhibitory interneurons expressing various calcium-binding proteins and neuropeptides. Moreover, grafting of hiPSC-MGE cells after SE mediated several neuroprotective and antiepileptogenic effects in the host hippocampus, as evidenced by reductions in host interneuron loss, abnormal neurogenesis, and aberrant mossy fiber sprouting in the dentate gyrus (DG). Furthermore, axons from graft-derived interneurons made synapses on the dendrites of host excitatory neurons in the DG and the CA1 subfield of the hippocampus, implying an excellent graft–host synaptic integration. Remarkably, seizure-suppressing effects of grafts were significantly reduced when the activity of graft-derived interneurons was silenced by a designer drug while using donor hiPSC-MGE cells expressing designer receptors exclusively activated by designer drugs (DREADDs). These results implied the direct involvement of graft-derived interneurons in seizure control likely through enhanced inhibitory synaptic transmission. Collectively, the results support a patient-specific MGE cell grafting approach for treating TLE.

EEG recordings | cognition and mood | GABA-ergic progenitors | medial ganglionic eminence | temporal lobe epilepsy

Hippocampal injury occurring from status epilepticus (SE) can lead to a state of chronic epilepsy, typified by spontaneous recurrent seizures (SRS) and cognitive and mood dysfunction (1–4). While treatment with antiepileptic drugs (AEDs) is efficacious for terminating SE in most cases, such treatment fails to curb epileptogenesis and the development of temporal lobe epilepsy (TLE) (5, 6). The long-term intake of AEDs is also linked to adverse side effects (7, 8). An alternative approach, such as cell therapy, has thus received considerable interest in treating TLE (9–11). Grafting of medial ganglionic eminence (MGE)-derived GABA-ergic progenitor cells has received significant attention in treating TLE for a variety of reasons. First, loss of GABA-ergic interneurons is a major pathological hallmark in TLE (12–15) and animal models of TLE (16, 17). Hence, enhancing inhibitory neurotransmission in the seizure foci by transplanted GABA-ergic neurons would restrain SRS. Second, virtually all MGE cells differentiate after grafting into one or other subclasses of GABA-ergic interneurons that are typically found in the intact hippocampus (18, 19). Third, the cells derived from MGE migrate well after grafting, become integrated into the hippocampal circuitry, enhance inhibitory neurotransmission in the hippocampus, and significantly suppress SRS (18–21).

Grafting of a variety of fetal cells into the hippocampus after SE has shown efficacy for decreasing seizures in the chronic phase (18, 19, 22–24). The extent of seizure suppression was considerably higher with fetal MGE cells, however (11). Furthermore, grafting of human MGE (hMGE)-like GABA-ergic progenitors derived from ES cells in a mouse model of TLE led to a reduction of SRS (25). Nonetheless, it is unclear if hMGE cell grafting can ease SRS in the long term, as only 5–10 d of electroencephalographic (EEG) recordings were employed to demonstrate seizure-suppressing

Significance

This study provides evidence that human induced pluripotent stem cell (hiPSC)-derived medial ganglionic eminence (MGE) cell grafting into the hippocampus after status epilepticus can greatly reduce the frequency of spontaneous seizures in the chronic phase through both antiepileptogenic and antiepileptic effects. The antiepileptogenic changes comprised reductions in host interneuron loss, abnormal neurogenesis, and aberrant mossy fiber sprouting, whereas the antiepileptic effects were evident from an increased occurrence of seizures after silencing of graft-derived interneurons. Additional curative impacts of grafting comprised improved cognitive and mood function. The results support the application of autologous human MGE cell therapy for temporal lobe epilepsy. Autologous cell therapy is advantageous as such a paradigm can avoid immune suppression and promote enduring graft–host integration.

Author contributions: D.U., D.J.P., and A.K.S. designed research; D.U., B.H., O.W.C., B.S., M.K., S.A., A.B., Y.D., and A.K.S. performed research; D.U., B.H., O.W.C., S.-C.Z., and A.K.S. analyzed data; and D.U., S.-C.Z., D.J.P., and A.K.S. wrote the paper.

Reviewers: D.B., Legacy Research Institute; and W.P.G., Institute of Psychological Medicine and Clinical Neurosciences.

The authors declare no conflict of interest.

[1]Present address: Centre for Molecular Neurosciences, Kasturba Medical College, Manipal Academy of Higher Education, Manipal, 576104 Karnataka, India.

[2]Present address: Institute Biological Sciences and Health, Federal University of Alagoas, Maceio, AL 57072-970, Brazil.

[3]S.-C.Z., D.J.P., and A.K.S. contributed equally to this work.

[4]To whom correspondence may be addressed. Email: shetty@medicine.tamhsc.edu or prockop@medicine.tamhsc.edu.

This article contains supporting information online at www.pnas.org/lookup/suppl/doi:10.1073/pnas.1814185115/-/DCSupplemental.

Published online December 17, 2018.

effects in a model known for SRS occurring in clusters separated by variable periods of no seizure activity (19). Currently, it is also unknown whether hMGE graft-derived cells are directly involved in the suppression of SRS. Importantly, for clinical translation, human induced pluripotent stem cell (hiPSC)-derived hMGE cells (26) appear more appropriate as such a paradigm not only overcomes ethical issues but also facilitates autologous or patient-specific hMGE cell therapy for TLE (27).

We generated human hMGE-like cells from hiPSCs through a rapid directed differentiation method and transplanted them into the hippocampus of rats that underwent kainate-induced SE, a well-characterized model of human TLE (28, 29). Using continuous EEG recordings for 21 d and a battery of behavioral tests, we demonstrate that grafting is effective in easing SRS as well as cognitive and mood impairments in the chronic phase of TLE. Importantly, through silencing of hMGE graft-derived neurons expressing designer receptors exclusively activated by designer drugs (DREADDs) with clozapine-*N*-oxide (CNO), we demonstrate that the therapeutic effect is achieved through modulation of local circuits by graft-derived GABA-ergic interneurons. Graft–host integration was also evident from robust survival, extensive migration and GABA-ergic differentiation of graft-derived cells, and synapse formation by graft-derived axons on hippocampal excitatory neurons.

Results

Grafting of hMGE Cells Suppress SRS in the Chronic Phase. SE was induced in 2-mo-old F344 rats as detailed in our previous report (30). Seven days later, animals were randomly assigned to an SE-alone group (n = 16), SE + grafts group (n = 12), SE + DREADDs graft group (n = 5), or SE + CNO group (n = 5). In the SE + grafts group, animals received grafts of standard hMGE cells (100,000 cells per site × 3), whereas in the SE + DREADDs graft group, animals received grafts of hMGE cells transduced with adeno-associated virus serotype 5 (AAV5) vectors carrying human-specific synaptophysin (hSyn)-hM4Di-mCherry DREADDs. In animals receiving transplants (i.e., SE + grafts, SE + DREADDs graft groups), daily cyclosporine A injections (10 mg/kg) were given starting 2 d before transplantation and continued until the experimental end point to avoid transplant rejection. In addition, to discern the effects of cyclosporine alone on the frequency of SRS, animals in the SE + CNO group received daily cyclosporine injections. The hMGE cells, generated from hiPSCs according to our previous protocol (31, 32), contained >92% cells expressing NKX2.1 (*SI Appendix*, Fig. S1*C*). The animals were examined for the frequency and intensity of SRS and for cognitive and mood function in the fifth month posttransplantation and for histological analysis in the sixth month postgrafting.

Continuous video-EEG recordings were made for 3 wk in the fifth month after SE. Comparison of data between the two groups revealed substantial reductions in frequencies of all SRS (72% reduction, $P < 0.0001$; Fig. 1*A1*) and stage V SRS (the most intense type of SRS, typified by bilateral forelimb clonus with rearing and falling; 78% reduction, $P < 0.0001$; Fig. 1*A2*) in the SE + grafts group. Although the average duration of individual SRS was similar between the two groups ($P > 0.05$; Fig. 1*A3*), the percentage of time spent in seizure activity for the recording period was considerably shorter in the SE + grafts group than in the SE-alone group (72% reduction, $P < 0.0001$; Fig. 1*A4*). Furthermore, analyses of data on a week-by-week basis for over 3 wk revealed consistent decreases in frequencies of all SRS ($P < 0.0001$; Fig. 1*B1*), stage V SRS ($P < 0.0001$; Fig. 1*B2*), and the percentage of time spent in seizure activity ($P < 0.0001$; Fig. 1*B4*) in every week. The average duration of individual SRS did not differ between the two groups, however ($P > 0.05$; Fig. 1*B3*), implying that when seizures occur in the grafted group, they lasted for a similar duration as seizures in the SE-alone group. Thus, bilateral grafting of hMGE cells into the hippocampus after SE considerably reduced the frequency and severity of SRS in the chronic phase of epilepsy.

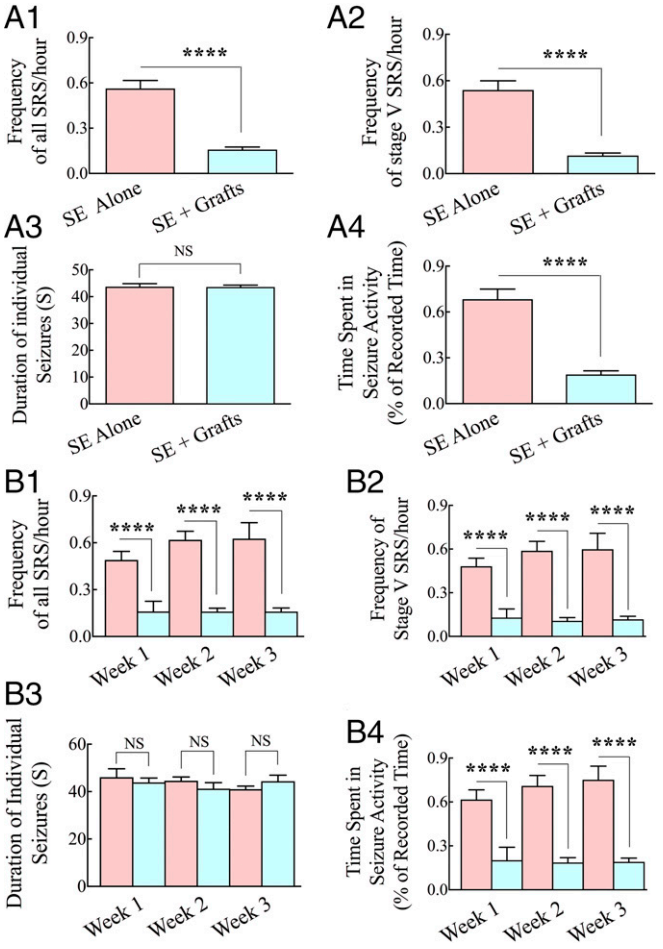

Fig. 1. hMGE-like cell grafting into the hippocampus after SE greatly restrained the frequency and intensity of SRS in the chronic phase. Data from 3 wk of continuous EEG recordings measured in the fifth month after SE are illustrated for the SE-alone and SE + grafts groups (n = 6 per group). The frequency of all SRS (*A1*), the frequency of stage V SRS (*A2*), the duration of individual SRS (*A3*), and the percentage of time spent in SRS activity (*A4*) are compared. ****$P < 0.0001$. Additional analyses of SRS activity on a week-by-week basis demonstrated consistent reductions in all SRS (*B1*), stage V SRS (*B2*), and the percentage of time spent in SRS activity (*B4*) over 3 wk. As shown in *A3* and *B3*, the duration of individual seizures was not different between the two groups in either analysis. ****$P < 0.0001$; NS, not significant.

hMGE Cell Grafting Reduces EEG Power in Both Ictal and Interictal Periods. In a blind analysis, 200 SRS with behavioral manifestations confirmed with video-EEG recordings (20 SRS per animal, n = 5 per group) were randomly chosen and analyzed for multiple spectral parameters. The average EEG power during ictal events (SRS) was significantly lower in the SE + grafts group than in the SE-alone group ($P < 0.001$; Fig. 2*A3*). There were no differences in the percentages of alpha and delta waves between the two groups (Fig. 2 *A4* and *A5*). However, the SE + grafts group displayed a reduced percentage of beta waves ($P < 0.001$; Fig. 2*A6*) and an increased percentage of theta waves ($P < 0.001$; Fig. 2*A7*). For spectral analysis in interictal periods, 30-min interictal segments devoid of noise signals were randomly chosen (four to 10 segments per animal, n = 5 per group). The average EEG power in interictal periods was significantly lower in the SE + grafts group than in the SE-alone group ($P < 0.001$; Fig. 2*B3*). However, significant differences were not seen for percentages of alpha, delta, beta, and theta waves (Fig. 2 *B4–B7*). Overall, in addition to greatly diminishing the frequency of SRS, hMGE grafting reduced the intensity of individual SRS as well as the EEG power in interictal periods.

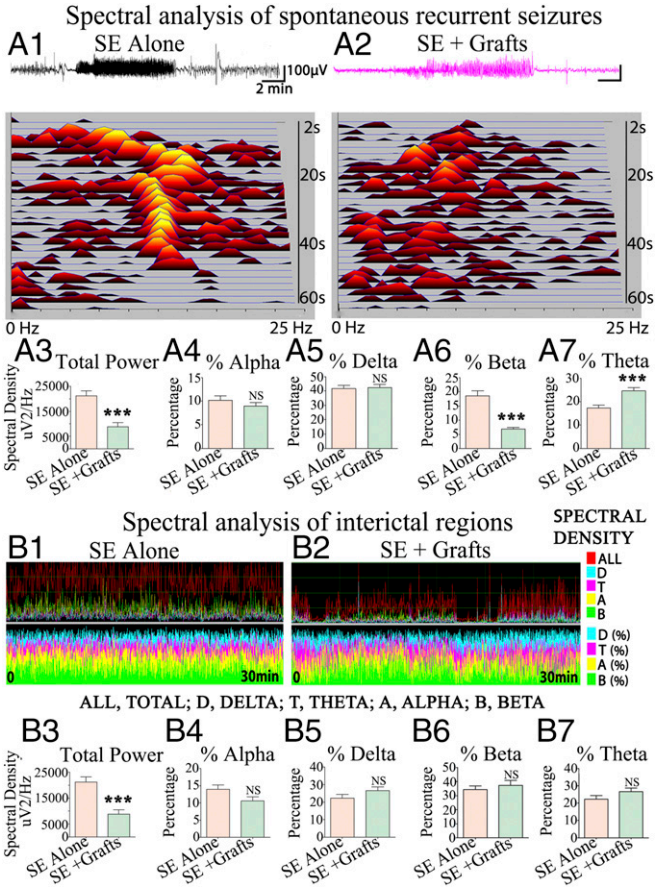

Fig. 2. Spectral analysis of SRS and interictal periods demonstrated reduced EEG power in animals receiving intrahippocampal grafts of hMGE-like cells after SE. Representative spectral densities seen during SRS in an animal from the SE-alone group (*A1*) and an animal from the SE + grafts group (*A2*) are illustrated. The average spectral density (*A3*) and alpha, delta, beta, and theta waves (*A4–A7*) are compared between the two groups (20 SRS per animal, $n = 5$ per group). Delta, theta, alpha, and beta wave activity during an interictal period in an animal from the SE-alone group (*B1*) and an animal from the SE + grafts group (*B2*) is illustrated. The average spectral density (*B3*) and percentages of alpha, delta, beta, and theta waves (*B4–B7*) are compared between the two groups (four to 10 interictal segments per animal, $n = 5$ per group). ***$P < 0.001$; NS, not significant.

hMGE Cell Grafting After SE Alleviates Cognitive and Pattern Separation Dysfunction. Cognitive impairment is a major comorbidity associated with chronic epilepsy. We first examined animals (naive, $n = 10$; SE-alone, $n = 10$; and SE + grafts, $n = 6$) with an object location test (OLT), a hippocampus-dependent test evaluating the cognitive aptitude to detect subtle changes in the immediate environment (33). Animals were examined for their proficiency to identify an object displaced to a new location (Fig. 3*A1*). Naive animals perceived a minor change in the environment by spending a greater amount of their object exploration time with the object displaced to a new location [novel place object (NPO)] than with the object in the familiar place [familiar place object (FPO)] ($P < 0.001$; Fig. 3*A2*). Animals in the SE-alone group displayed impairment in this task by showing a comparable propensity to explore both an NPO and an FPO ($P > 0.05$; Fig. 3*A3*). Animals in the SE + grafts group exhibited similar behavior as naive animals by showing a higher affinity to explore an NPO vis-à-vis an FPO ($P < 0.01$; Fig. 3*A4*). Comparative data on the total object exploration time, the distance traveled, and the mean velocity of movement between different groups are available in *SI Appendix*, Fig. S2 *A1–A3*.

We next examined the proficiency of animals for pattern separation, a capacity to discriminate similar but not identical experiences through storage of representations in a nonoverlapping manner (34, 35). Following the exploration of the open field (trial 1), each animal consecutively explored two different sets of identical objects (object types 1 and 2) placed on distinct types of floor patterns [pattern types 1 and 2 (P1 and P2)] in acquisition trials 2 and 3 (Fig. 3*B1*). In the testing phase (trial 4), each animal explored an object from trial 3 [which is now a familiar object (FO)] and an object from trial 2 [which is now a novel object (NO)] placed on the floor pattern employed in trial 2 (P2). Naive animals displayed normal pattern separation ability by showing a greater affinity for exploration of the NO on P2 ($P < 0.0001$; Fig. 3*B2*). Animals in SE were impaired, which was evident from their exploration of the NO and FO on P2 for nearly equal periods ($P > 0.05$; Fig. 3*B3*). Animals in the SE + grafts group, in contrast, exhibited similar behavior as naive animals by exploring the NO for greater periods than the FO ($P < 0.05$; Fig. 3*B4*), implying the preservation of pattern separation ability. Differences in other parameters, such as the total object exploration time, the distance traveled, and the mean velocity of movement between groups, are illustrated in the *SI Appendix*, Fig. S2 *B1–B3*.

We also probed whether animals that received hMGE grafts after SE retained recognition memory function using a novel object recognition test (NORT), a test dependent primarily on the integrity of the perirhinal cortex and partially on the hippocampus (33). The ability of animals to recognize an NO over an FO was examined (*SI Appendix*, Fig. S2*C1*). Naive animals showed normal recognition memory function by spending a more significant amount of their object exploration time within the novel object area (NOA) than within the familiar object area (FOA; $P < 0.001$; *SI Appendix*, Fig. S2*C2*). Animals in the SE-alone group exhibited recognition memory dysfunction by exploring the NOA and FOA for nearly equal times ($P > 0.05$; *SI Appendix*, Fig. S2*C3*). Conversely, animals in the SE + grafts group showed intact recognition memory function by exploring the NOA for a longer amount of time than the FOA ($P < 0.001$; *SI Appendix*, Fig. S2*C4*) in trial 3.

Collectively, the results of the three behavioral tests described above implied that animals receiving hMGE cell grafts after SE displayed a better ability for solving cognitive, pattern separation, and recognition memory tasks than SE-alone animals in the chronic phase.

hMGE Cell Grafting Eases Motivational Deficits and Anhedonia. Mood dysfunction is another comorbidity linked to chronic epilepsy. Animals in all groups (naive, $n = 10$; SE-alone, $n = 10$; and SE + grafts, $n = 6$) were first examined for the extent of motivation to eat food following 24-h food deprivation (a measure of depression) using an eating-related depression test (ERDT), which is a modified version of the novelty suppressed feeding test (NSFT) (36, 37). The reason for choosing the ERDT over the NSFT for examining depressive-like behavior in epileptic rats is described in our earlier report (32) and *SI Appendix*. The test was conducted in the home cage instead of a novel open-field box to reduce anxiety. The average latency to reach and smell food in SE-alone group was 10-fold longer than in the naive control group ($P < 0.001$; Fig. 3*C1*), implying a significantly decreased motivation in SE-alone animals. Latencies to reach and smell food in the SE + grafts group were significantly shorter than in the SE-alone rats ($P < 0.001$) but closer to those in naive animals ($P > 0.05$) (Fig. 3*C1*). Analyses of the latency to the first bite of food also showed similar results (Fig. 3*C2*). Thus, animals in the SE + grafts group showed a level of motivation that was closer to naive animals.

Since chronic epilepsy is also associated with anhedonia (i.e., inability to feel pleasure in activities that offer comfort in normal conditions), we employed a sucrose preference test (SPT). This test provides a measure of mood function in rodent prototypes from their preference for sweet fluids over regular water (38, 39). The absence of anhedonia in naive animals was evident from their choice for consuming a more significant amount of sucrose solution than water, which resulted in a considerably higher sucrose preference rate (SPR; ~80%; Fig. 3 *D1–D3*). The presence

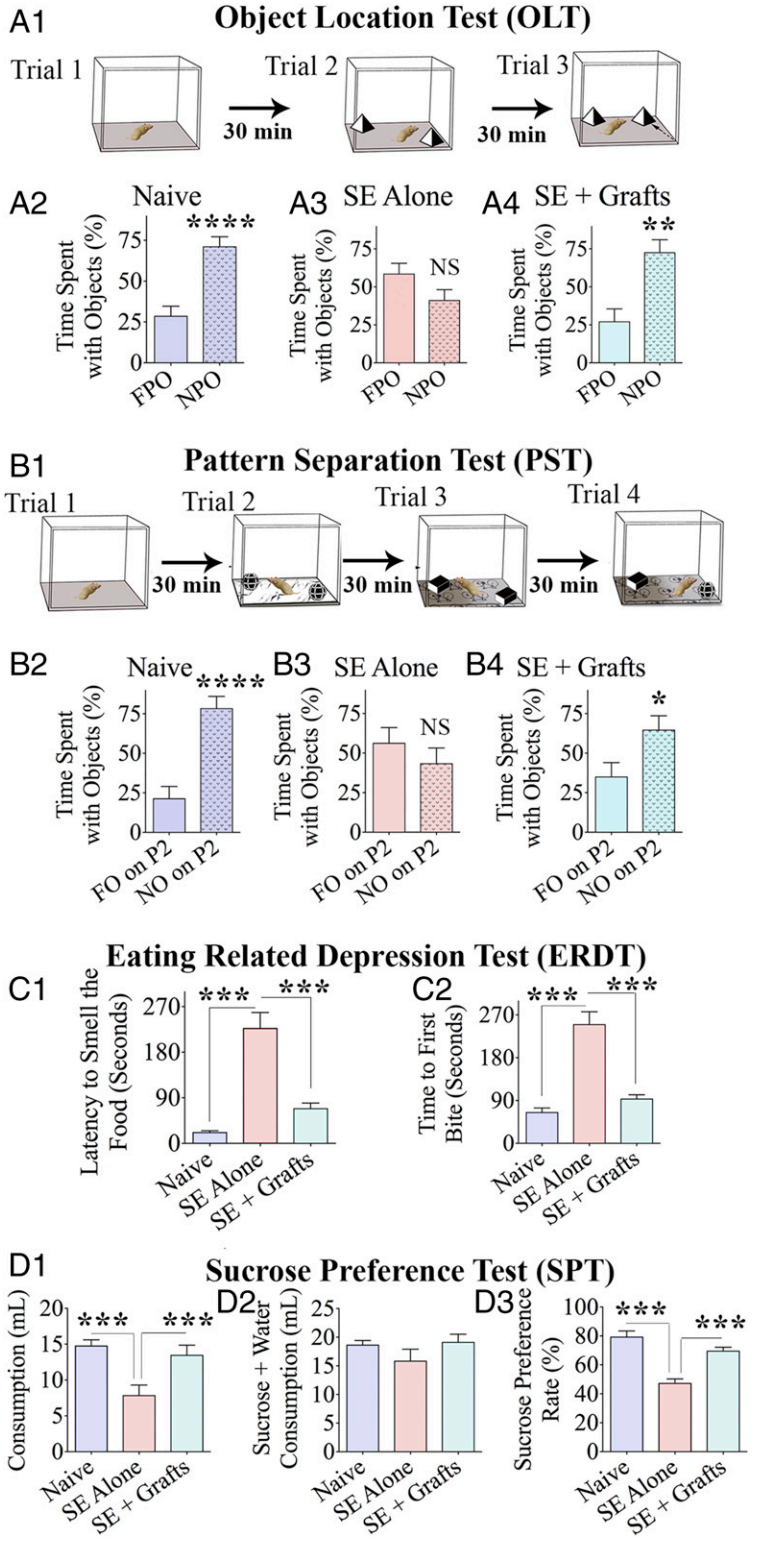

Fig. 3. hMGE-like cell grafting into the hippocampus after SE maintained better cognitive and mood function in the chronic phase. The various phases (trials) involved in an OLT (*A1*) and a pattern separation test (PST; *B1*) are graphically depicted. (*A2–A4* and *B2–B4*) Bar charts compare percentages of time spent with different objects (n = 6–10 per group). Bar charts compare latencies to smell food (*C1*) and the first bite of food (*C2*) in an ERDT between the three groups of animals (n = 6–10 per group). (*D1–D3*) Bar charts show data from a sucrose preference test (SPT), which is a test for measuring anhedonia. The bar chart in *D2* compares the amount of total liquid (sucrose + water) consumption between groups. *$P < 0.05$; **$P < 0.01$; ***$P < 0.001$; ****$P < 0.0001$; NS, not significant.

of anhedonia in SE-alone animals was apparent from the consumption of sucrose solution and water in almost equal amounts (SPR < 50%; Fig. 3 *D1–D3*). In contrast, animals in the SE + grafts group exhibited comparable behavior as naive animals by consuming a higher amount of sucrose solution (SPR ~ 70%, $P < 0.0001$; Fig. 3 *D1–D3*), indicating no anhedonia. The results were not influenced

by differences in the overall consumption of fluids in the testing period, as the total consumption (i.e., sucrose-containing water + regular water) was comparable between groups (Fig. 3*D2*).

hMGE Cells Survive and Migrate Extensively. Examination of sections through the hippocampus immunostained for human nuclear antigen (HNA) revealed that cells derived from hMGE cell grafts survived well. Grafts appeared healthy, as dead cell debris was rarely observed. Also, signs of lymphocyte infiltration were absent in graft cores or the host hippocampus in samples stained for HNA and DAPI, implying that daily s.c. cyclosporine injections effectively prevented graft rejection through immune suppression. The number of graft-derived cells in the entire hippocampus was stereologically measured using serial sections. The total number of live cells initially grafted into each hippocampus was ∼300,000 cells (i.e., ∼100,000 live cells in three sites). Quantification suggested a yield of 386,015 ± 20,882 graft-derived cells per hippocampus (n = 5), which is equivalent to ∼129% of injected cells. Increased yield than initially grafted implied proliferation of some graft-derived cells. Furthermore, graft-derived cells migrated pervasively into different regions and cell layers of the hippocampus (Fig. 4 *A1* and *B1*), including the subgranular zone and dentate hilus of the dentate gyrus (DG) (Fig. 4 *A2* and *B2*) and the stratum oriens, stratum pyramidale, and stratum radiatum of the CA1 subfield (Fig. 4 *A1* and *A3*) and the CA3 subfield (Fig. 4*A4*). Additional images showing extensive migration of graft-derived cells are presented in *SI Appendix*, Fig. S3.

hMGE Cells Differentiate Primarily into GABA-ergic Interneurons. A series of dual-immunofluorescence staining for HNA (a marker of human cells) with various neural cell markers was performed (n = 5). Then, using Z-section analysis in a confocal microscope, percentages of different cell types among HNA^+ cells were measured. This analysis revealed that the majority of graft-derived cells (HNA^+ cells) differentiated into neuron-specific nuclear antigen-positive ($NeuN^+$) mature neurons (87%; Fig. 5 *A1–A3*) and, more specifically, into GABA-ergic interneurons (76%; Fig. 5 *B1–B3*). Further characterization using markers of various subclasses of GABA-ergic interneurons revealed differentiation of graft-derived cells into interneurons expressing parvalbumin (PV; 27%; Fig. 5 *C1–C3*) and neuropeptide Y (NPY; 11%; Fig. 5 *D1–D3*). Smaller percentages of graft-derived cells also differentiated into interneurons expressing somatostatin (SS; 6%; Fig. 5 *E1–E3*) and calretinin (CR; 8%; Fig. 5 *F1–F3*). Similar differentiation was also apparent in graft-derived cells that migrated away from the graft core. A few examples are shown in *SI Appendix*, Fig. S4 *A1–B3*. Interestingly, graft-derived NPY^+ and SS^+ interneurons were seen mostly in smaller clusters (*SI Appendix*, Fig. S4 *C1–D2*), suggesting that specific clones of $NKX2.1^+$ cells may have generated these interneurons. Analysis of graft-derived cells with markers of glia revealed the presence of a small number of $GFAP^+$ astrocytes (3%; *SI Appendix*, Fig. 5 *G1–G3*). However, $O1/O4^+$ oligodendrocytes or neuron-glia protein 2^+ ($NG2^+$) oligodendrocyte progenitors were absent (Fig. 5 *H1–H3*).

Minority of Cells in hMGE Grafts Display Proliferation and Neural Progenitor Markers. The core of grafts was larger in a majority of animals likely because of some proliferation occurring after grafting. Evaluation of graft-derived cells using HNA and Ki67 dual immunofluorescence 5 mo after grafting showed that <1% of graft-derived cells were proliferating (n = 5; *SI Appendix*, Fig. S5 *A1–A3*), implying that most proliferation occurred in the early phase after grafting. A small number of graft-derived cells retained expression of the neuronal progenitor marker Sox-2 (8%, n = 5; *SI Appendix*, Fig. S5 *B1–B3*). Nestin expression was seen in the soma of only 4% of graft-derived cells, but processes of many graft-derived cells retained nestin expression (n = 5; *SI Appendix*, Fig. S5 *C1–C3*). Nonetheless, teratoma formation was not seen in any of the grafted animals. Furthermore, none of the graft-derived cells expressed the pluripotent stem cell markers Oct-4, TRA-1-81, or SSEA3, implying that all grafted cells had committed to a neural lineage. Moreover, the presence of cholinergic neurons expressing choline acetyltransferase, another neuronal type derived from $NKX2.1^+$ cells in defined culture conditions and after grafting into the hippocampus following a cholinergic lesion in the medial septum (40), was rarely seen among graft-derived cells (<1%; *SI Appendix*, Fig. S5 *D1–D3*). This implied that $NKX2.1^+$ cells used in this study were primed for differentiation primarily into GABA-ergic interneurons.

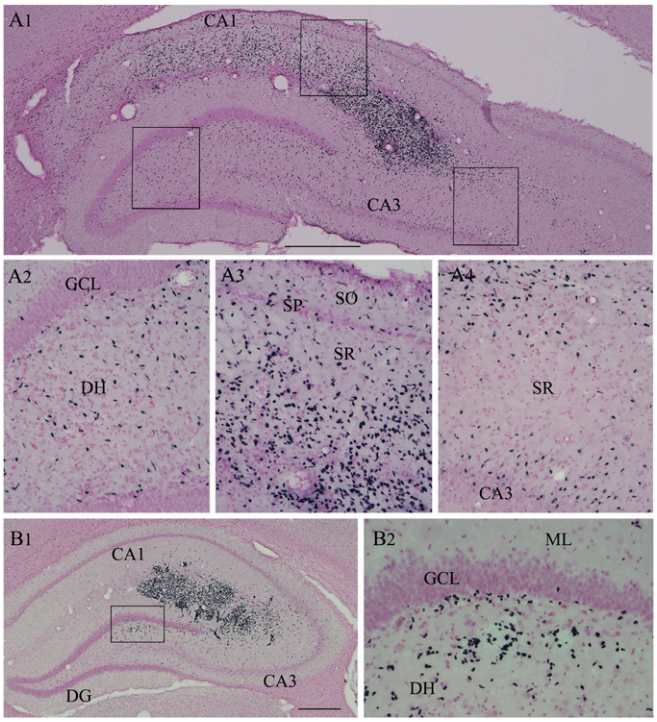

Fig. 4. Cells derived from hMGE-like cell grafts placed into the hippocampus after SE pervasively migrated to different subfields and layers of the hippocampus. (*A1*) Example of migration of cells from an hMGE graft core located at the end of the hippocampal fissure. Magnified views of regions from *A1* showing the extensive migration of graft-derived cells into the dentate hilus (*A2*), the CA1 subfield (*A3*), and the CA3 subfield (*A4*) are shown. (*B1* and *B2*) Another example of robust migration of cells into the DH from an hMGE graft core located in the hippocampal fissure and the adjoining CA1 and CA3 subfields. DH, dentate hilus; ML, molecular layer; SGZ, subgranular zone; SO, stratum oriens; SP, stratum pyramidale; SR, stratus radiatum. (Scale bars: *A1*, 400 μm; *B1*, 200 μm; *A2–A4* and *B2*, 100 μm.)

hMGE Cell Grafting Reduces Abnormal Neurogenesis. We measured the long-term effect of hMGE grafting after SE on neurogenesis occurring 5 mo after SE and grafting (n = 5 per group). Through stereological quantification of doublecortin-positive (DCX^+) neurons, we measured both normal neurogenesis [i.e., newly born neurons in the subgranular zone-granule cell layer (GCL)] and abnormal neurogenesis (i.e., newly born neurons in the dentate hilus) (Fig. 6 *A1–A5*). The extent of normal neurogenesis was significantly reduced in the SE-alone group in comparison to the age-matched naive group ($P < 0.001$; Fig. 6 *A1*, *A2*, and *A4*). Animals in the SE + grafts group displayed higher levels of normal neurogenesis than animals in the SE-alone group ($P < 0.001$; Fig. 6 *A2–A4*), although the overall neurogenesis remained less than in the naive group ($P < 0.001$; Fig. 6 *A1–A4*). Furthermore, animals in the SE-alone group displayed newly born neurons in the dentate hilus (i.e., aberrant neurogenesis). The amount of aberrant neurogenesis was reduced in the SE + grafts group in comparison to the SE-alone group ($P < 0.01$; Fig. 6 *A2*, *A3*, and *A5*). Since reelin is involved in guiding the migration of newly born neurons into the GCL (41), we measured

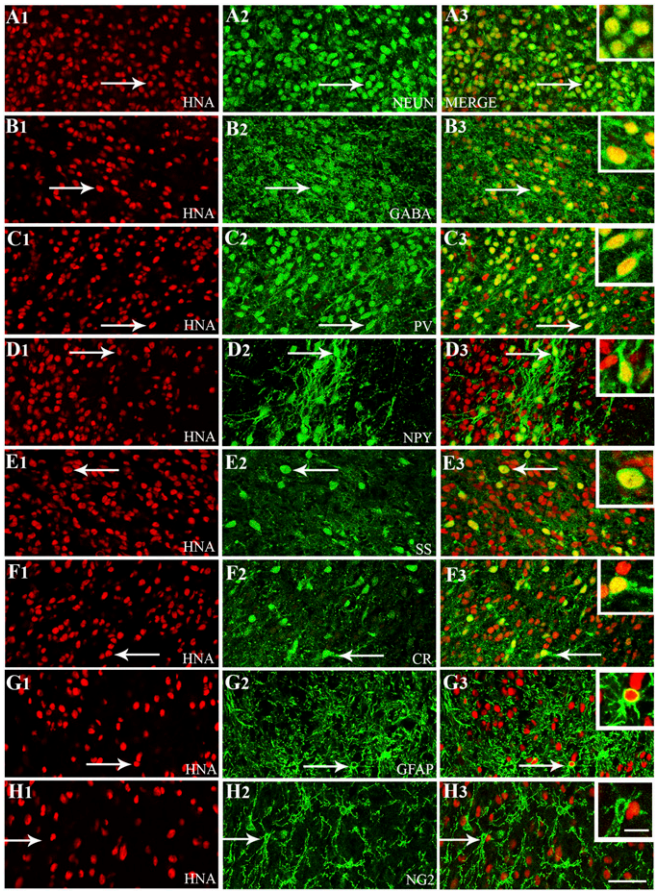

Fig. 5. Cells derived from hMGE-like cell grafts placed into the hippocampus after SE differentiated predominantly into GABA-expressing interneurons comprising various subclasses. Differentiation of hMGE graft-derived cells into neurons expressing neuron-specific nuclear antigen (NeuN; *A1–A3*) and interneurons expressing GABA (*B1–B3*) is illustrated. Differentiation of hMGE graft-derived cells into subclasses of interneurons expressing PV (*C1–C3*), NPY (*D1–D3*), SS (*E1–E3*), and calretinin (CR; *F1–F3*) is illustrated. (*G1–H3*) Differentiation of hMGE graft-derived cells into GFAP$^+$ astrocytes is minimal, and none of the hMGE graft-derived cells differentiate into neuron-glia 2$^+$ (NG2$^+$) oligodendrocyte progenitors. All cells in red (first column) denote graft-derived cells expressing HNA (a marker of human cells), whereas cells in green (second column) illustrate cells expressing neuronal or glial antigens. The third column illustrates merged images from columns 1 and 2. Arrows in *A1–G3* denote examples of dual-labeled cells, whereas arrows in *H1–H3* denote a host NG2$^+$ cell. (*Insets*) In the third column, magnified views of cells indicated by arrows are displayed. (Scale bars: *A1–H3*, 50 μm; *Insets*, 20 μm.)

the numbers of surviving reelin$^+$ interneurons in the dentate hilus. The reelin$^+$ interneuron number was significantly reduced in the SE-alone group in comparison to the naive group ($P < 0.001$; Fig. 6 *B1*, *B2*, and *B4*). Animals in the SE + grafts group displayed more significant numbers of reelin$^+$ interneurons than animals in the SE-alone group ($P < 0.001$; Fig. 6 *B2–B4*), although the overall number remained less than in the naive group ($P < 0.001$; Fig. 6 *B1*, *B3*, and *B4*). Thus, hMGE cell grafting after SE facilitated the maintenance of normal hippocampal neurogenesis at higher levels with better preservation of reelin$^+$ interneurons.

hMGE Cell Grafting Preserves Greater Numbers of Host GABA-ergic Interneurons. We performed stereological quantification of interneurons expressing PV, NPY, and SS 5 mo after SE ($n = 5$ per group) to uncover the long-term effects of hMGE grafting on total interneuron numbers in the DG. In comparison to the naive group, animals in the SE-alone group displayed decreased numbers of PV$^+$, NPY$^+$, and SS$^+$ interneurons ($P < 0.01$–0.001; Fig. 6 *C1–E4*). In animals belonging to the SE + grafts group, the numbers of these interneurons were comparable to those of animals in the naive group ($P > 0.05$; Fig. 6 *C1–E4*) and more significant than those of animals in the SE-alone group ($P < 0.05$–0.001; Fig. 6 *C1–E4*). In the SE + grafts group, to ascertain the actual host interneuron number per DG, we deducted numbers of specific interneurons derived from grafts. Numbers of PV$^+$, NPY$^+$, and SS$^+$ interneurons derived from grafts in the DG were quantified using data such as the total number of graft-derived cells in the DG and percentages of PV$^+$, NPY$^+$, and SS$^+$ interneurons among graft-derived cells. These numbers are illustrated in *SI Appendix*, Fig. S6 *A1–A3*), which showed that grafting of hMGE cells after SE led to better preservation of host PV$^+$ and NPY$^+$ interneurons in the DG. Moreover, when combined with graft-derived interneurons, numbers of PV$^+$, NPY$^+$, and SS$^+$ interneurons in the DG of the SE + grafts group either

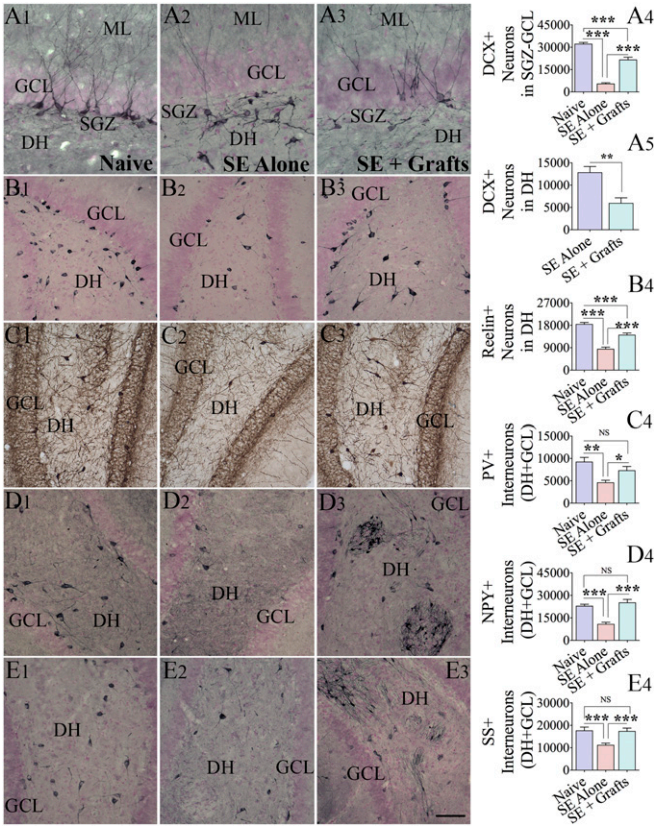

Fig. 6. hMGE-like cell grafting after SE maintained higher levels of normal neurogenesis with reduced abnormal neurogenesis and diminished the loss of various subclasses of host interneurons. Distribution and density of DCX$^+$ newly born neurons in the subgranular zone (SGZ)-GCL and the dentate hilus (DH) (*A1–A3*) and reelin$^+$ interneurons in the DH (*B1–B3*) from representative animals belonging to naive (first column), SE-alone (second column), and SE + grafts (third column) groups are illustrated. Bar charts compare numbers of DCX$^+$ neurons in the SGZ-GCL (*A4*; normal neurogenesis) and the DH (*A5*; abnormal neurogenesis). (*B4*) Bar chart compares the number of reelin$^+$ interneurons between different groups ($n = 5$ per group). The distribution and density of interneurons expressing PV (*C1–C3*), NPY (*D1–D3*), and SS (*E1–E3*) in the DH and GCL of representative animals belonging to naive (first column), SE-alone (second column), and SE + grafts (third column) groups are illustrated. Arrows in *D3* and *E3* denote clusters of NPY$^+$ and SS$^+$ interneurons derived from hMGE grafts. (*C4*, *D4*, and *E4*) Bar charts compare numbers of PV$^+$, NPY$^+$, and SS$^+$ interneurons in DH + GCL between different groups ($n = 5$ per group). The numbers include both graft-derived interneurons and host interneurons in these charts. The numbers of host interneurons only are shown in *SI Appendix*, Fig. S6. ML, molecular layer; NS, not significant. *$P < 0.05$; **$P < 0.01$; ***$P < 0.001$. (Scale bars: *A1–A3*, 100 μm; *B1–B3*, *C1–C3*, *D1–D3*, and *E1–E3*, 200 μm.)

equaled or exceeded numbers in the naive control group (Fig. 6 *C1–E4*).

hMGE Cell Grafting Reduces Aberrant Mossy Fiber Sprouting. Progressively increasing sprouting of granule cell axons into the inner molecular layer of the DG, also referred to as aberrant mossy fiber sprouting (MFS), is one of the signs of conspicuous abnormal axonal plasticity seen after SE and in patients with TLE (42, 43). Although aberrant MFS has been correlated with the extent of DG hyperexcitability in previous studies, its contribution to the occurrence of SRS is controversial (44, 45). We quantified the extent of MFS 5 mo after SE, using zinc transporter 3 immunostaining and densitometry analysis ($n = 5$ per group). The extent of MFS in the SE-alone group was moderate in the upper blade of the DG but extensive in the lower blade of the DG (*SI Appendix*, Fig. S7 *A1* and *B1*). In the SE + grafts group, reduced sprouting was evident in both blades of the DG, in comparison to the SE-alone group (*SI Appendix*, Fig. S7 *A1–C3*). The reductions were significant for the lower blade of the DG, as well as when the DG was taken in its entirety ($P < 0.05$–0.01; *SI Appendix*, Fig. S7 *C2* and *C3*).

Therapeutic Effect Is Substantially Reduced When the Activity of Graft-Derived Neurons Is Inhibited. We performed an additional experiment using hMGE cells transduced with AAV-hSyn-hM4D(Gi)-mCherry as donor cells for grafting ($n = 5$) to ascertain the contribution of graft-derived GABA-ergic interneurons in reducing SRS activity in the SE + grafts group. In the chronic phase after SE and grafting, EEG recordings were taken for 4 d without the activation of DREADDs, followed by 4 d of EEG recordings with activation of DREADDs through injections of CNO every 8 h. EEG recordings were performed for an additional 4 d, commencing 2 d after the CNO washout period. All parameters of SRS, such as frequencies of all SRS and stage V SRS and the percentage of time spent in seizure activity, were at lower levels in EEG recordings taken during the pre-CNO administration period. This pattern of reduced SRS activity is consistent with the effects of hMGE grafting for suppressing SRS, as presented in Fig. 1, implying that the seizure-suppressant impact mediated by DREADDs expressing hiPSC-MGE cells is similar to that of the naive hiPSC-MGE cells. An apparent surge in all parameters of SRS was observed in EEG recordings taken during the period of activation of DREADDs by CNO ($P < 0.05$; Fig. 7 *A1–A3*). In contrast, EEG recordings obtained 2 d after the CNO washout period revealed a pattern of SRS activity that was similar to the pre-CNO period ($P > 0.05$; Fig. 7 *A1–A3*) but weaker than during the CNO administration period ($P < 0.05$; Fig. 7 *A1–A3*). Evaluation of grafts of hMGE cells transduced with AAV-hSyn-hM4D (Gi)-mCherry using triple immunofluorescence for microtubule-associated protein (MAP-2; a marker of neurons), mCherry (reflecting the expression of DREADDs), and HNA (a marker of graft-derived cells) revealed the presence of mCherry in neurons derived from hMGE grafts (Fig. 7 *B1–B4*). Approximately 74% of graft-derived neurons expressed mCherry, although the extent of expression varied in different cells and mCherry expression seemed to be restricted mostly to the soma of neurons (Fig. 7*C*). Thus, increased frequency of SRS after activation of DREADDs correlated with expression of DREADDs in graft-derived neurons. However, the overall incidence of SRS after silencing of graft-derived interneurons (Fig. 7 *A1–A3*) did not reach the rate of SRS seen in the SE-alone animals (Fig. 1 *A1*, *A2*, and *A4*), implying that some of the reductions in SRS frequency are due to antiepileptogenic changes mediated by grafts.

To clarify whether cyclosporine alone or CNO alone has effects on SRS activity in epileptic animals, we performed EEG recordings in SE-alone rats ($n = 5$). These animals received daily s.c. cyclosporine injections from post-SE day 5 until the start of CNO injections. As described for animals in the SE + grafts group, EEG recordings were taken for 4 d before the commencement of CNO injections, for 4 d during CNO injections (once every 8 h), and for 4 d after the CNO washout period (commencing 2 d after the last CNO injection). Measurement of SRS parameters (frequencies of all SRS and stage V SRS and the time spent in seizure activity) before CNO injections revealed that daily s.c. cyclosporine injections commencing from the fifth day after SE and continuing for several months do not have any effect on the frequency and intensity of SRS occurring in the chronic phase of epilepsy (Fig. 7 *D1–D3*). Importantly, the SRS parameters in these animals were highly comparable to SRS parameters observed in the SE-alone animals that did not receive daily cyclosporine (Fig. 1 *A1*, *A2*, and *A4*). These results also imply that long-term cyclosporine administration did not influence SRS parameters in animals receiving hMGE cell grafts.

Additionally, no significant differences were observed in SRS parameters between pre-CNO, CNO, and post-CNO periods ($P > 0.05$;

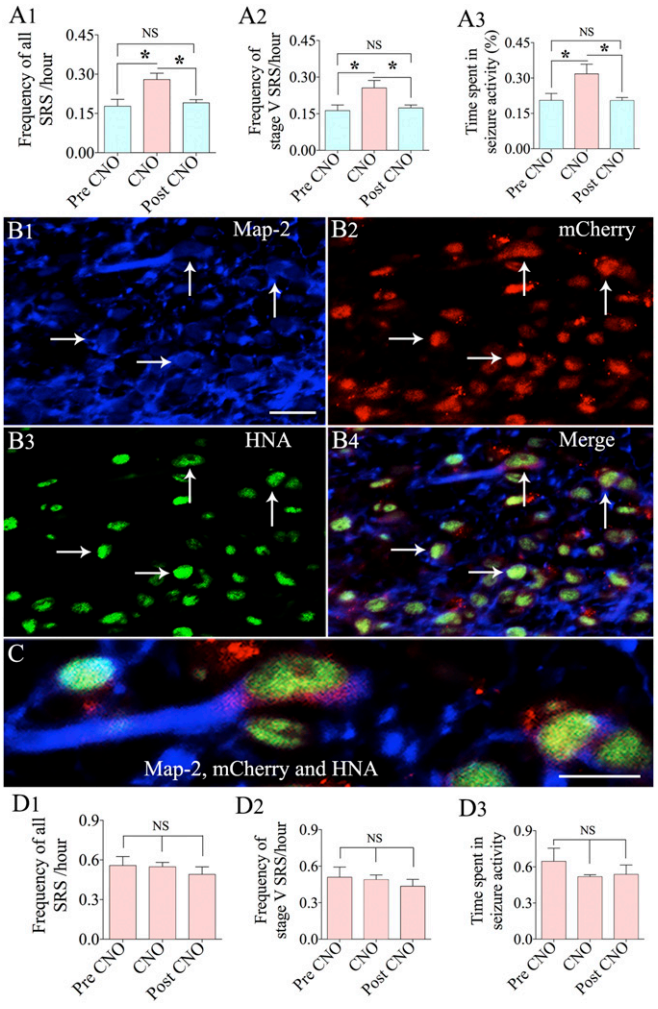

Fig. 7. Analysis using hMGE-like cells labeled with DREADDs as donor cells confirmed that graft-derived GABA-ergic interneurons contributed to the suppression of seizures in animals receiving hMGE grafts after SE. Bar charts compare frequencies of all SRS (*A1*) and stage V SRS (*A2*) and the percentage of time spent in SRS activity for the recording period (*A3*) in continuous EEG recordings taken during different periods of CNO administration in animals receiving grafts of hMGE cells transduced with AAV-hSyn-hM4D(Gi)-mCherry after SE ($n = 5$). Images of triple immunofluorescence for MAP-2 (a marker of neurons; *B1*, blue), mCherry (reflecting the expression of DREADDs; *B2*, red), and HNA (a marker of graft-derived cells; *B3*, green) are shown, demonstrating the presence of mCherry in neurons derived from hMGE grafts (indicated by arrows). (*B4*) Merged image showing all three colors. (*B4* and *C*) mCherry expression was mostly restricted to the soma of neurons. (*D1–D3*) Bar charts compare the effects of CNO administration on SRS activity in SE-alone animals ($n = 5$). NS, not significant. *$P < 0.05$. (Scale bars: *B1–B4*, 20 μm; *C*, 10 μm.)

Fig. 7 *D1–D3*), implying that CNO administration has no effects on SRS in chronically epileptic animals. These results reinforce that the functional incorporation of graft-derived GABA-ergic interneurons into the hippocampal circuitry is one of the primary mechanisms underlying reduced SRS activity in grafted animals.

Synapse Formation Between Graft-Derived Axons and Host Excitatory Neurons. A significantly enhanced frequency of SRS following silencing of graft-derived GABA-ergic interneurons expressing DREADDs implied connectivity between hMGE graft-derived GABA-ergic interneuron axons and the host excitatory neurons. To confirm this, we employed Z-section analyses in a confocal microscope following triple immunofluorescence of hippocampal sections for hSyn, postsynaptic density protein-95 (PSD-95), and MAP-2 or beta-III tubulin (TuJ-1). The presence of both pre- and postsynaptic puncta (hSyn and PSD-95) was confirmed in two consecutive 1-μm-thick optical sections (or two adjacent optical sections). This characterization showed the formation of synapses by graft-derived axons on the host granule cell dendrites in the DG (Fig. 8 *A1–A3*), as well as on the host CA1 pyramidal neuron dendrites in the CA1 stratum radiatum (Fig. 8 *B1–C3*). Synapses were evident from direct contacts between hSyn-expressing graft-derived axon endings and PSD-95–expressing regions on host excitatory neuron dendrites expressing MAP-2 (Fig. 8*A3*) or TuJ-1 (Fig. 8*C3*). Some graft-derived axons also made synapses on the soma of dentate granule cells (Fig. 8*A3*). These results suggest that synaptic integration of graft-derived GABA-ergic interneurons with the host excitatory neurons underlay the reduced SRS and improved cognitive and mood function observed in epileptic animals receiving hMGE cell grafts. An increased incidence of SRS seen with silencing of graft-derived GABA-ergic interneurons expressing DREADDs supports this conclusion.

Discussion

The results of this study provide evidence for the therapeutic efficacy of hiPSC-derived hMGE cells in alleviating the progression of SE-induced injury into a state of chronic epilepsy. Substantially diminished frequency and intensity of SRS linked with reduced EEG power in interictal periods, improved location and recognition memory and pattern separation function, and alleviation of mood dysfunction comprised the curative effects of grafts. By grafting hMGE cells that are engineered to express DREADDs, we have shown that the therapeutic effect is primarily achieved by regulating the local inhibitory circuitry in the hippocampus. Furthermore, synapses made by graft-derived GABA-ergic interneurons on the dendrites of host excitatory neurons in the DG and the CA1 subfield provided additional proof for graft–host synaptic integration. Also, grafting of hiPSC-MGE cells early after SE reduced host interneuron loss, abnormal neurogenesis, and aberrant MFS, while promoting normal neurogenesis.

Continuous video-EEG recordings for 21 d in the chronic phase of TLE demonstrate that hiPSC-derived hMGE cell grafting after SE considerably restrained SRS. A previous study has shown the efficacy of human ES-derived MGE-like cell grafts for easing SRS in a mouse pilocarpine model of TLE (25). However, in that study, the authors employed only 5–10 d of EEG recordings, which is not sufficient to validate the seizure-suppressing effects of grafts, as SRS can occur in clusters over days or weeks in this mouse model of epilepsy (25). Our week-by-week analysis demonstrated consistently reduced SRS over 3 wk in grafted epileptic animals and perpetuation of an equal frequency of SRS in epileptic animals receiving no grafts. Vitally, an experiment analyzing the functional integration of grafts showed that graft-derived neurons were implicated in reducing SRS in the chronic phase. Direct involvement of grafts was evident from significantly increased SRS activity with silencing of graft-derived GABA-ergic interneurons through CNO-mediated activation of hM4Di (a DREADDs receptor) expressed on them. Furthermore, the formation of synapses by axon endings of graft-derived GABA-ergic interneurons on the soma and dendrites of host DG granule cells and dendrites of the host CA1 pyramidal neurons suggested that synaptic integration of graft-derived GABA-ergic interneurons with the host excitatory neurons underlay the reduced SRS.

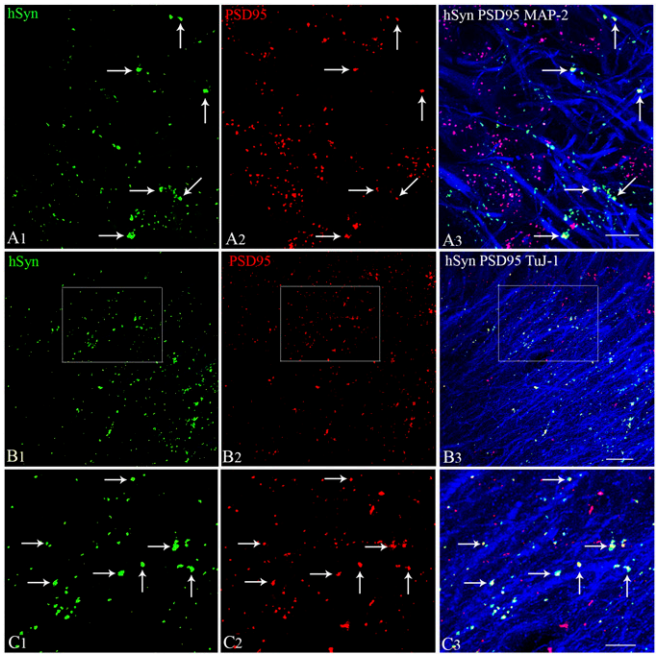

Fig. 8. Synapse formation between graft-derived axons and host hippocampal excitatory neurons in the DG and the CA1 subfield. Synapses between hSyn-expressing axon endings from graft-derived neurons (*A1*, green) and PSD-95–expressing regions (*A2*, red) on MAP-2 positive dendrites of DG granule cells (*A3*, blue) are illustrated. Direct contacts between $hSyn^+$ and $PSD\text{-}95^+$ structures show the location of synapses on DG granule cell dendrites (indicated by arrows in *A3*). Synapses between $hSyn^+$ axon endings from graft-derived neurons (*B1*, green) and $PSD\text{-}95^+$ regions (*B2*, red) on $TuJ\text{-}1^+$ dendrites of CA1 pyramidal neurons (*B3*, blue) are illustrated. (*C1–C3*) Magnified views of areas from *B1–B3* showing synaptic contacts between graft-derived $hSyn^+$ presynaptic terminals on $PSD95^+$ postsynaptic regions in the host hippocampal CA1 pyramidal neuron dendrites. Two 1-μm-thick consecutive optical sections (two adjacent sections) were employed to confirm the presence of both pre- and postsynaptic puncta (hSyn- and PSD95-stained structures) on dendrites. (Scale bars: *A1–A3* and *C1–C3*, 10 μm; *B1–B3*, 20 μm.)

A much reduced frequency of SRS in grafted animals can result from both antiepileptogenic and antiepileptic effects of grafts. Concerning the occurrence of SRS, all animals in the SE + grafts group displayed greatly diminished frequency of SRS in comparison to SE-only animals, suggesting that the hippocampus became less epileptogenic after hiPSC-MGE cell grafting, and hence could generate fewer SRS in the chronic phase. Moreover, significantly reduced EEG power seen during interictal periods indirectly implied reduced hyperexcitability of neurons in grafted animals because spike activity in interictal periods can lead to a seizure when neurons reach a specific spatial and temporal density. On the other hand, the direct antiepileptic effect of graft-derived interneurons was evidenced from an increased occurrence of SRS after silencing of graft-derived interneurons in the DREADDs study. However, the fact that the overall frequency of SRS after silencing of graft-derived interneurons did not reach the rate of SRS seen in SE-alone animals indicates that some of the reductions in SRS frequency are due to antiepileptogenic changes mediated by grafts. Thus, significantly reduced frequency of SRS in the SE + grafts group is a result of both antiepileptogenic effects of grafting and the direct antiepileptic impact of graft-derived interneurons through increased inhibitory neurotransmission.

The antiepileptogenic impact of grafts comprised protection of host GABA-ergic interneurons, reduced abnormal neurogenesis

with the maintenance of higher levels of normal neurogenesis, and lessened aberrant MFS. Moderation of these abnormal changes is noteworthy because the extent of some of these epileptogenic changes can influence the frequency of SRS in TLE (12, 14, 15, 45–47). Reduced loss of host interneurons with grafting may be due to neuroprotective properties of grafted NKX2.1$^+$ cells, as immature progenitor cells are known to release a variety of neurotrophic factors as well as to enhance the levels of endogenous neurotrophic factors (24). Maintenance of higher levels of normal neurogenesis, along with diminished aberrant neurogenesis in grafted animals, is likely linked to the better preservation of NPY$^+$ and reelin$^+$ interneurons observed in the DG. These possibilities are based on the role of NPY in regulating hippocampal NSC proliferation and on the role of reelin in promoting a regular pattern of neurogenesis by guiding the migration of newly born neurons into the GCL (41, 48, 49). Furthermore, abated MFS may be the result of decreased abnormal neurogenesis, as a significant amount of MFS after SE has been suggested to arise from aberrantly integrated newly born granule cells (50).

In addition to SRS activity, cognitive and mood impairments are other features of chronic TLE (1, 2, 4, 30). In this study, animals receiving hMGE grafts after SE showed better cognitive and mood function than SE-alone animals. Cognitive and mood impairments in chronic epilepsy are likely a result of frequent seizure activity (51, 52), as well as reduced normal neurogenesis and persistence of abnormal neurogenesis (53, 54). Frequent seizure activity and enhanced interictal spike activity may interfere with the synchronized activity of excitatory and inhibitory neurons required for cognitive function or memory formation (55). Likewise, associations between the extent of normal hippocampal neurogenesis and cognitive and mood function have been seen in multiple previous studies (56–58). Furthermore, ablating abnormal neurogenesis after SE improves memory function in epileptic animals (46), and reduced hippocampal neural stem cell activity is linked to memory dysfunction in patients with epilepsy (59). Thus, better cognitive and mood function in epileptic animals receiving hMGE grafts is ostensibly a consequence of both reduced SRS activity and maintenance of normal neurogenesis at higher levels with reduced abnormal neurogenesis.

The promise of primary MGE cells to reduce SRS in distinct animal models of epilepsy has been recognized for some time, from studies using MGE cells from the rodent fetal brain (18, 19) and MGE cells generated from human ES cells (25). Nonetheless, development of MGE cell therapy for patients with epilepsy has not received much traction because of the nonavailability of appropriate donor cells. The use of human fetal MGE cells is impractical due to ethical issues and the difficulty in obtaining the required amount of human fetal MGE tissues. Application of MGE cells from human ES cells, although less contentious ethically than fetal cells (60), still requires immune suppression for prolonged periods after grafting, which may cause unpleasant side effects and slow graft rejection over time. The current results using hiPSC-derived hMGE cell grafts is significant from this standpoint, as this approach allows autologous hMGE cell grafting; hence, long-term immune suppression after grafting is likely not required. Autologous cell therapy likely promotes an enduring integration of graft-derived neurons with the host hippocampus (27), providing a long-lasting treatment for TLE. Furthermore, teratoma formation was not observed in this study, although smaller fractions of graft-derived cells displayed proliferative activity and expressed markers of neural progenitor cells at ∼5 mo postgrafting. Importantly, none of the graft-derived cells expressed pluripotent stem cell markers, implying that all grafted cells had committed to a neural lineage. Nonetheless, for clinical translation, it would be necessary to employ purified, postmitotic MGE cells derived from hiPSCs to rule out the possibility of tumor formation. Moreover, for clinical translation in patients with drug-resistant TLE, the effects of hiPSC-MGE cell grafting into the hippocampus in the chronic phase of epilepsy (i.e., when the animals are exhibiting robust and consistent SRS over months) on SRS and related comorbidities will need to be critically evaluated.

Methods

Animals and Induction of SE. All experiments were performed as per the animal protocol, approved by the Institutional Animal Care and Use Committee of the Texas A&M Health Sciences Center and Central Texas Veterans Health Care System. SE was induced in 2-mo-old male F344 rats, using graded i.p. injections of kainic acid. The procedure is detailed in our earlier reports (30) and in *SI Appendix*. Following SE, animals were randomly assigned to the SE-alone group (n = 16), SE + grafts group (n = 12), SE + DREADDs graft group (n = 5), and SE + CNO group (n = 5). In the SE + grafts group, animals received grafts of standard hMGE cells, whereas in the SE + DREADDs graft group, animals received grafts of hMGE cells transduced with AAV5 vectors carrying hSyn-hM4Di-mCherry DREADDs. A group of age-matched naive control rats (n = 10) was also included for comparison of behavioral and histological results.

Generation of NKX2.1$^+$ MGE Progenitors from hiPSCs and Grafting. NKX2.1-expressing hMGE cells were generated from hiPSCs (IMR90-4; Wisconsin International Stem Cell Bank), as described previously (31, 32). Cells were grafted ∼35 d after neural induction. For functional analysis of grafts, DREADDs expressing hMGE cells were used as donor cells. For this, neurospheres were dissociated into smaller cell aggregates, maintained in neural induction medium containing sonic hedgehog for 24 h, and transduced with AAV5-hSyn-hM4Di-mCherry (Bryan Roth laboratory, University of North Carolina Vector Core) for 48 h. Cells were washed thoroughly by repeated centrifugation to remove dead cells and to obtain >85% viable cells. In all grafting experiments, cell suspensions were primed with a neural differentiation medium comprising 1 μM cAMP and 10 ng/mL each of BDNF, GDNF, and IGF-1. The transplantation procedure is described in our previous report (61) and in *SI Appendix*.

Implantation of Electrodes, EEG Recordings, and Analyses of SRS. Implantation of EEG electrodes was performed in the fourth month after SE. The procedure employed is described in our previous report (29) and in *SI Appendix*. In the fifth month after SE, animals were connected to a tethered video-EEG system for continuous EEG recordings for 3 wk. The video-EEG system continuously monitored simultaneously occurring behavior and electrographic activity in freely behaving subgroups of animals belonging to the SE-alone (n = 6) and SE + grafts (n = 6) groups. EEG tracings from these animals were next analyzed for the frequency of all SRS, the frequency of stage V SRS, the average duration of individual SRS, and the percentage of time spent in seizure activity for the recording period. A detailed blind spectral analysis was performed for 200 randomly selected seizures (20 SRS per animal, n = 5 per group). Furthermore, four to 10 randomly selected 30-min interictal segments were analyzed in each animal for spectral density (n = 5 per group). Animals in the SE + grafts group receiving AAV5-hSyn-hM4Di-mCherry–transduced hMGE cells (n = 5) and SE-alone rats receiving CNO (n = 5) were monitored with continuous EEG recordings for 4 d in each of the following three time segments: (*i*) before CNO injections (pre-CNO period), (*ii*) during CNO injections (CNO period), and (*iii*) 2 d after the last CNO injection (post-CNO period). The drug CNO was injected at 3 mg/kg once every 8 h for 4 d.

Evaluation of Cognitive and Mood Function Using Behavioral Tests. Age-matched naive control animals (n = 10) and subgroups of animals from the SE-alone group (n = 10) and SE + grafts group (n = 6) were subjected to multiple behavioral tests for assessing cognitive and mood function in the fifth month after SE. Cognitive function was assessed through three object-based tests, which included an OLT, pattern separation test, and NORT, whereas mood function was evaluated through an ERDT (a modified version of the NSFT) and SPT. The protocols employed in these behavioral tests are detailed in our previous reports (32, 62) and in *SI Appendix*.

Brain Tissue Processing, and Immunohistochemistry. Following completion of EEG recordings and behavioral tests, animals were euthanized and brain tissues were harvested. The procedures for the harvesting of fixed brain tissues, immunohistochemistry for neural antigens, and stereological quantification of graft-derived cells and various host cell types are detailed in *SI Appendix*.

Dual/Triple-Immunofluorescence Methods and Confocal Microscopy. The procedures employed for phenotypic analyses of grafts using dual/triple-immunofluorescence methods and Z-section analysis using a confocal microscope are described in our earlier reports (24, 61) and in *SI Appendix*.

Statistical Analysis. Statistical analyses were performed using Prism software (GraphPad). One-way ANOVAs with Newman–Keuls multiple comparison post hoc tests were employed when three groups were compared. Comparison within groups in the behavioral tests or comparison between the two groups (e.g., DCX counts in DG) were performed using unpaired, two-tailed Student's

t tests. Numerical data were presented as mean ± SEM, and $P < 0.05$ was considered statistically significant.

ACKNOWLEDGMENTS. This work was supported by grants from the Department of Defense [Grant W81XWH-14-1-0558 (to A.K.S.)], the State of Texas [Emerging Technology Fund (to A.K.S.)], and the Department of Veterans Affairs [Merit Award I01BX000883 and BLR&D Research Career Scientist Award 1IK6BX003612 (to A.K.S.)], as well as the NIH/National Institute of Neurological Disorders and Stroke (Grants NS086604 and NS096282) and NIH/National Institute of Mental Health [Grant MH100031 (to S.-C.Z.)].

1. Dudek FE, Hellier JL, Williams PA, Ferraro DJ, Staley KJ (2002) The course of cellular alterations associated with the development of spontaneous seizures after status epilepticus. *Prog Brain Res* 135:53–65.
2. Dingledine R, Varvel NH, Dudek FE (2014) When and how do seizures kill neurons, and is cell death relevant to epileptogenesis? *Adv Exp Med Biol* 813:109–122.
3. Goldberg EM, Coulter DA (2013) Mechanisms of epileptogenesis: A convergence on neural circuit dysfunction. *Nat Rev Neurosci* 14:337–349.
4. Seinfeld S, Goodkin HP, Shinnar S (2016) Status epilepticus. *Cold Spring Harb Perspect Med* 6:a022830.
5. Löscher W, Brandt C (2010) Prevention or modification of epileptogenesis after brain insults: Experimental approaches and translational research. *Pharmacol Rev* 62: 668–700.
6. Trinka E, Brigo F, Shorvon S (2016) Recent advances in status epilepticus. *Curr Opin Neurol* 29:189–198.
7. Cramer JA, et al. (2011) Non-interventional surveillance study of adverse events in patients with epilepsy. *Acta Neurol Scand* 124:13–21.
8. Chen B, et al. (2017) Psychiatric and behavioral side effects of antiepileptic drugs in adults with epilepsy. *Epilepsy Behav* 76:24–31.
9. Maisano X, et al. (2012) Differentiation and functional incorporation of embryonic stem cell-derived GABAergic interneurons in the dentate gyrus of mice with temporal lobe epilepsy. *J Neurosci* 32:46–61.
10. Shetty AK (2014) Hippocampal injury-induced cognitive and mood dysfunction, altered neurogenesis, and epilepsy: Can early neural stem cell grafting intervention provide protection? *Epilepsy Behav* 38:117–124.
11. Shetty AK, Upadhya D (2016) GABA-ergic cell therapy for epilepsy: Advances, limitations and challenges. *Neurosci Biobehav Rev* 62:35–47.
12. de Lanerolle NC, Kim JH, Robbins RJ, Spencer DD (1989) Hippocampal interneuron loss and plasticity in human temporal lobe epilepsy. *Brain Res* 495:387–395.
13. Marco P, et al. (1996) Inhibitory neurons in the human epileptogenic temporal neocortex. An immunocytochemical study. *Brain* 119:1327–1347.
14. Spreafico R, et al. (1998) Cortical dysplasia: An immunocytochemical study of three patients. *Neurology* 50:27–36.
15. Löscher W, Gernert M, Heinemann U (2008) Cell and gene therapies in epilepsy–Promising avenues or blind alleys? *Trends Neurosci* 31:62–73.
16. Hirsch JC, et al. (1999) Deficit of quantal release of GABA in experimental models of temporal lobe epilepsy. *Nat Neurosci* 2:499–500.
17. Kobayashi M, Buckmaster PS (2003) Reduced inhibition of dentate granule cells in a model of temporal lobe epilepsy. *J Neurosci* 23:2440–2452.
18. Hunt RF, Girskis KM, Rubenstein JL, Alvarez-Buylla A, Baraban SC (2013) GABA progenitors grafted into the adult epileptic brain control seizures and abnormal behavior. *Nat Neurosci* 16:692–697.
19. Henderson KW, et al. (2014) Long-term seizure suppression and optogenetic analyses of synaptic connectivity in epileptic mice with hippocampal grafts of GABAergic interneurons. *J Neurosci* 34:13492–13504.
20. Baraban SC, et al. (2009) Reduction of seizures by transplantation of cortical GABAergic interneuron precursors into Kv1.1 mutant mice. *Proc Natl Acad Sci USA* 106: 15472–15477.
21. Casalia ML, Howard MA, Baraban SC (2017) Persistent seizure control in epileptic mice transplanted with gamma-aminobutyric acid progenitors. *Ann Neurol* 82:530–542.
22. Rao MS, Hattiangady B, Rai KS, Shetty AK (2007) Strategies for promoting anti-seizure effects of hippocampal fetal cells grafted into the hippocampus of rats exhibiting chronic temporal lobe epilepsy. *Neurobiol Dis* 27:117–132.
23. Hattiangady B, Rao MS, Shetty AK (2008) Grafting of striatal precursor cells into hippocampus shortly after status epilepticus restrains chronic temporal lobe epilepsy. *Exp Neurol* 212:468–481.
24. Waldau B, Hattiangady B, Kuruba R, Shetty AK (2010) Medial ganglionic eminence-derived neural stem cell grafts ease spontaneous seizures and restore GDNF expression in a rat model of chronic temporal lobe epilepsy. *Stem Cells* 28:1153–1164.
25. Cunningham M, et al. (2014) hPSC-derived maturing GABAergic interneurons ameliorate seizures and abnormal behavior in epileptic mice. *Cell Stem Cell* 15:559–573.
26. Nicholas CR, et al. (2013) Functional maturation of hPSC-derived forebrain interneurons requires an extended timeline and mimics human neural development. *Cell Stem Cell* 12:573–586.
27. Du X, Parent JM (2015) Using patient-derived induced pluripotent stem cells to model and treat epilepsies. *Curr Neurol Neurosci Rep* 15:71.
28. Hellier JL, Patrylo PR, Buckmaster PS, Dudek FE (1998) Recurrent spontaneous motor seizures after repeated low-dose systemic treatment with kainate: Assessment of a rat model of temporal lobe epilepsy. *Epilepsy Res* 31:73–84.
29. Rao MS, Hattiangady B, Reddy DS, Shetty AK (2006) Hippocampal neurodegeneration, spontaneous seizures, and mossy fiber sprouting in the F344 rat model of temporal lobe epilepsy. *J Neurosci Res* 83:1088–1105.
30. Hattiangady B, Shetty AK (2011) Neural stem cell grafting in an animal model of chronic temporal lobe epilepsy. *Curr Protoc Stem Cell Biol* Chapter 2:Unit2D.7.
31. Liu Y, et al. (2013) Directed differentiation of forebrain GABA interneurons from human pluripotent stem cells. *Nat Protoc* 8:1670–1679.
32. Upadhya D, et al. (2016) Neural stem cell or human induced pluripotent stem cell-derived GABA-ergic progenitor cell grafting in an animal model of chronic temporal lobe epilepsy. *Curr Protoc Stem Cell Biol* 38:2D.7.1–2D.7.47.
33. Hattiangady B, et al. (2014) Object location and object recognition memory impairments, motivation deficits and depression in a model of Gulf War illness. *Front Behav Neurosci* 8:78.
34. Leutgeb JK, Leutgeb S, Moser MB, Moser EI (2007) Pattern separation in the dentate gyrus and CA3 of the hippocampus. *Science* 315:961–966.
35. Yassa MA, Stark CE (2011) Pattern separation in the hippocampus. *Trends Neurosci* 34: 515–525.
36. Samuels BA, Hen R (2011) Neurogenesis and affective disorders. *Eur J Neurosci* 33: 1152–1159.
37. Powell TR, Fernandes C, Schalkwyk LC (2012) Depression-related behavioral tests. *Curr Protoc Mouse Biol* 2:119–127.
38. Willner P, Muscat R, Papp M (1992) Chronic mild stress-induced anhedonia: A realistic animal model of depression. *Neurosci Biobehav Rev* 16:525–534.
39. Snyder JS, Soumier A, Brewer M, Pickel J, Cameron HA (2011) Adult hippocampal neurogenesis buffers stress responses and depressive behaviour. *Nature* 476:458–461.
40. Liu Y, et al. (2013) Medial ganglionic eminence-like cells derived from human embryonic stem cells correct learning and memory deficits. *Nat Biotechnol* 31:440–447.
41. Gong C, Wang TW, Huang HS, Parent JM (2007) Reelin regulates neuronal progenitor migration in intact and epileptic hippocampus. *J Neurosci* 27:1803–1811.
42. Sutula T, Cascino G, Cavazos J, Parada I, Ramirez L (1989) Mossy fiber synaptic reorganization in the epileptic human temporal lobe. *Ann Neurol* 26:321–330.
43. Shetty AK, Turner DA (1999) Aging impairs axonal sprouting response of dentate granule cells following target loss and partial deafferentation. *J Comp Neurol* 414: 238–254.
44. Dudek FE, Obenaus A, Schweitzer JS, Wuarin JP (1994) Functional significance of hippocampal plasticity in epileptic brain: Electrophysiological changes of the dentate granule cells associated with mossy fiber sprouting. *Hippocampus* 4:259–265.
45. Buckmaster PS (2014) Does mossy fiber sprouting give rise to the epileptic state? *Adv Exp Med Biol* 813:161–168.
46. Cho KO, et al. (2015) Aberrant hippocampal neurogenesis contributes to epilepsy and associated cognitive decline. *Nat Commun* 6:6606.
47. Hosford BE, Liska JP, Danzer SC (2016) Ablation of newly generated hippocampal granule cells has disease-modifying effects in epilepsy. *J Neurosci* 36:11013–11023.
48. Howell OW, et al. (2005) Neuropeptide Y stimulates neuronal precursor proliferation in the post-natal and adult dentate gyrus. *J Neurochem* 93:560–570.
49. Howell OW, et al. (2007) Neuropeptide Y is important for basal and seizure-induced precursor cell proliferation in the hippocampus. *Neurobiol Dis* 26:174–188, and erratum (2013) 49:199.
50. Kron MM, Zhang H, Parent JM (2010) The developmental stage of dentate granule cells dictates their contribution to seizure-induced plasticity. *J Neurosci* 30:2051–2059.
51. Kanner AM (2016) Psychiatric comorbidities in epilepsy: Should they be considered in the classification of epileptic disorders? *Epilepsy Behav* 64:306–308.
52. Stewart E, Catroppa C, Lah S (2016) Theory of mind in patients with epilepsy: A systematic review and meta-analysis. *Neuropsychol Rev* 26:3–24.
53. Hattiangady B, Rao MS, Shetty AK (2004) Chronic temporal lobe epilepsy is associated with severely declined dentate neurogenesis in the adult hippocampus. *Neurobiol Dis* 17:473–490.
54. Hattiangady B, Shetty AK (2010) Decreased neuronal differentiation of newly generated cells underlies reduced hippocampal neurogenesis in chronic temporal lobe epilepsy. *Hippocampus* 20:97–112.
55. Lenck-Santini PP, Scott RC (2015) Mechanisms responsible for cognitive impairment in epilepsy. *Cold Spring Harb Perspect Med* 5:a022772.
56. Lazarov O, Hollands C (2016) Hippocampal neurogenesis: Learning to remember. *Prog Neurobiol* 138–140:1–18.
57. Anacker C, Hen R (2017) Adult hippocampal neurogenesis and cognitive flexibility–Linking memory and mood. *Nat Rev Neurosci* 18:335–346.
58. Peng L, Bonaguidi MA (2018) Function and dysfunction of adult hippocampal neurogenesis in regeneration and disease. *Am J Pathol* 188:23–28.
59. Coras R, et al. (2010) Low proliferation and differentiation capacities of adult hippocampal stem cells correlate with memory dysfunction in humans. *Brain* 133: 3359–3372.
60. Aach J, Lunshof J, Iyer E, Church GM (2017) Addressing the ethical issues raised by synthetic human entities with embryo-like features. *eLife* 6:e20674, and erratum (2017) 6:e27642.
61. Shetty AK, Hattiangady B (2016) Grafted subventricular zone neural stem cells display robust engraftment and similar differentiation properties and form new neurogenic niches in the young and aged hippocampus. *Stem Cells Transl Med* 5:1204–1215.
62. Long Q, et al. (2017) Intranasal MSC-derived A1-exosomes ease inflammation, and prevent abnormal neurogenesis and memory dysfunction after status epilepticus. *Proc Natl Acad Sci USA* 114:E3536–E3545.